Korean J. Chem. Eng., **29**(5), 574-582 (2012)
DOI: 10.1007/s11814-011-0217-z

Effects of burner type on a bench-scale entrained flow gasifier and conceptual modeling of the system with Aspen Plus

Joongwon Lee†, Seik Park, Haikyung Seo, Miyeong Kim, Simoon Kim, Junhwa Chi, and Kitae Kim

Power Generation Lab., KEPCO Research Institute, 65 Munji-ro, Yuseong-gu, Daejeon 305-760, Korea
(*Received 22 March 2011 • accepted 18 August 2011*)

Abstract−The integrated gasification combined cycle (IGCC) system is well known for its high efficiency compared with that of other coal fueled power generating systems. In this study, gasification using different types of burners with different oxygen supply angles in a bench-scale entrained flow gasifier was investigated. The effects of the oxygen gas supply angle of the coal burner and resulting oxygen supply location in the gasifier on the syngas composition and temperature of the gasifier were experimentally examined. These changes had a significant influence on the syngas composition of the final stream, carbon conversion, and efficiencies. According to the experimental results, the models using the Aspen Plus process simulator were positioned to define the effects of the experimental parameters and to find the optimum operating conditions in the bench gasifier facility.

Key words: Gasification, Entrained Flow Gasifier, Aspen Plus, Modeling

INTRODUCTION

Coal gasification is a versatile process that can convert a solid fuel to syngas, which can be further converted and separated into hydrogen, which is a valuable and environmentally acceptable energy carrier. The core of gasification plants is the gasifier, which can be realized in very different configurations and solutions. There are three general types of gasifier: an entrained bed, a moving bed, and a fluidized bed. Integrated gasification combined cycle (IGCC) systems have usually been based on entrained gasifiers due to their fuel flexibility, their production of high pressure steam, and the lack of tar in the produced gas. Entrained gasifiers are operated in a slagging mode and most are oxygen blown. Steam is also usually required if the coal is not fed as a water slurry [1].

Although gasification is a relatively old process, the versatility of the process and multiplicity of technology solutions causes it to continue to be an important topic for investigation. A further motivation for the renewed interest in this technology is the combination of gasification with advanced operation of gas clean up and storage such as carbon capture and storage (CCS). The IGCC models that optimize and analyze the system that are found in the literature are usually validated with data from existing plants. The most recent works on IGCC, especially gasification systems, are summarized in Table 1 [2-15].

Despite all these differences, many processes that were studied in the literature [5-7,13,14] have modeled the gasifier as an equilib-

Table 1. Current state of IGCC modeling

Author/Year	Feed material	Bed type	Simulation tool	State
Wen and Chaung, 1979	Liquefied coal	Entrained	-	Steady
Govind and Shah, 1984	Liquefied coal	Entrained	-	Steady
Higman and Van der Burgt, 2003	Solid carbon	General	-	Steady/Dynamic
Frey and Akunuri, 2001	Coal	Entrained	Aspen Plus (Gibbs)	Steady
Martinez and Vicente, 2006	Petcoke	Entrained	Matlab (Gibbs)	Steady
Nather and Kirkpatrick, 2008	Coal	Entrained	Hysys (Gibbs)	Steady
Chen and Horio, 2000	Coal	Entrained	-	Dynamic
Brown and Fuchino, 2005	Biomass	Fluidized	-	Steady
Valero and Uson, 2002	Coal+Petcoke+Biomass	Entrained	Engineering equation solver	Steady
Petersen and Werther ,2005	Sewage sludge	Circulating fluidized	Programming language: C	Steady
Robinson and Luyben, 2008	Biomass+Coal	Fluidized	Aspen dynamics	Dynamic
Biagini and Bardi, 2009	Coal	Entrained	Hysys+Aspen Plus	Steady
Perez-Fortes and Bojarski, 2009	Coal	Entrained	Aspen Plus	Steady
Lee and Kim, 2010	Coal	Entrained	Aspen Plus	Steady

†To whom correspondence should be addressed.
E-mail: joongwonlee@kepco.co.kr

rium reactor. This approach is indeed fundamental and sufficient for a preliminary study, but it is unsuitable for process analysis and optimization. To develop a rigorous model of the gasification reactor while minimizing the number of hypotheses, the gasification reactor was divided into three simulated reactors in this study, and it was assumed that pyrolysis, volatile combustion, and char gasification occurred individually in each reactor. A plug flow reactor (PFR) was used in the char gasification. This is desirable because the need for the assumption that the gasifier is in an equilibrium condition with a constant temperature is nullified.

The model was validated with experimental data taken from the bench plant which is located in the Korea Electronic Power Corporation (KEPCO) Research Institute. The effects of the oxygen supply angle and the gasifier burner location on the carbon conversion and product gas composition were investigated.

EXPERIMENTAL SECTION

1. Reactor Description

Fig. 1 is a schematic diagram of the gasifier facility [16,17].

The facility consists of three components: a feeding system, a gasifier system, and cleaning parts (wet-scrubbing system, desulfurizer system, flare stack system). The feeding system is upstream of coal burner. The coal in the receiver hopper is in a dry condition and ready to be used; it is transferred to the lock hopper through the cyclone via nitrogen transfer gas. The coal feed rate was quantitatively controlled by the screw feeder. The gasification system is comprised of the gasifier and the coal burner. A bench scale coal gasifier was designed to maintain up to 10 bar and 1,500 °C; the maximum coal feed rate was 1 ton per day. The final component of the facility is the gas cleaning parts comprised of a wet scrubber, a desulfurizer, and a flare stack to burn up the syngas. The top and middle sections of the gasifier are lined with refractory material designed to withstand the operating temperature. In these sections, the pyrolysis, combustion, and gasification reactions occur. Also, the lower section has a quench section. The bottom water level was maintained at all times through continuous injections of the cooling water. The gasifier design and the 1 ton per day gasification system are shown in Fig. 2 and Fig. 3.

The gasifier is connected with nitrogen feed, oxygen feed, coal feed, and product gas lines. The coal and oxygen are fed to the gasifier after being heated with another fuel (LPG) and maintained at a tem-

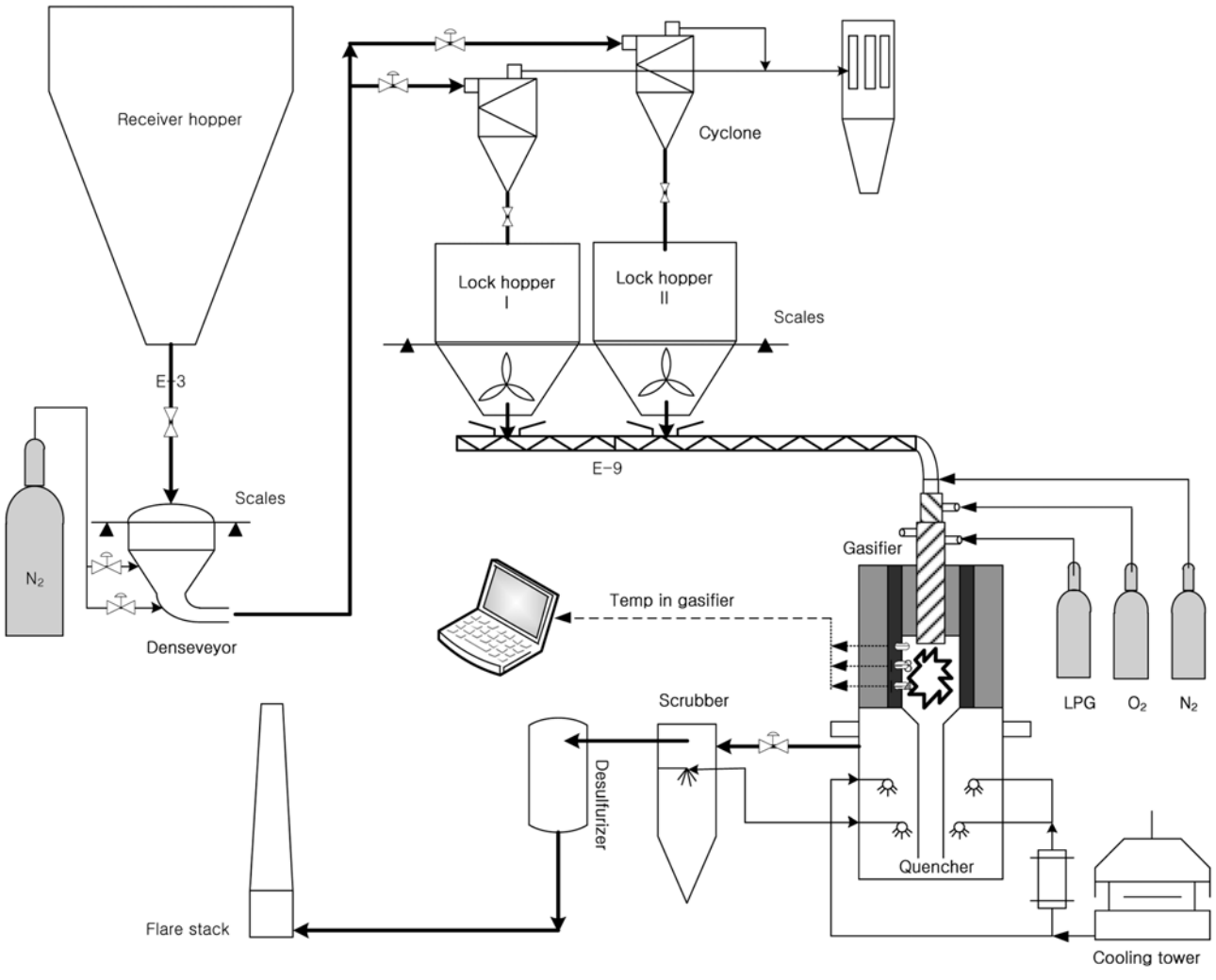

Fig. 1. Schematic diagram of the gasifier facility.

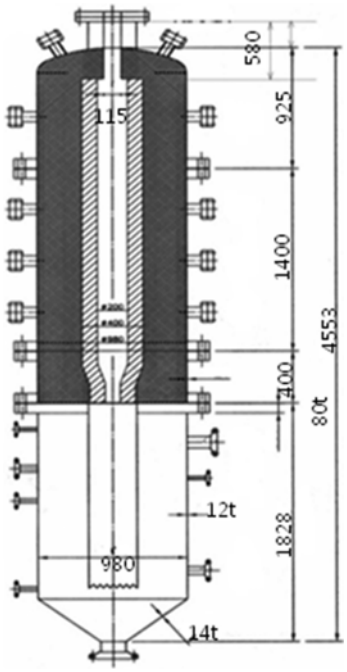

Fig. 2. Gasifier design.

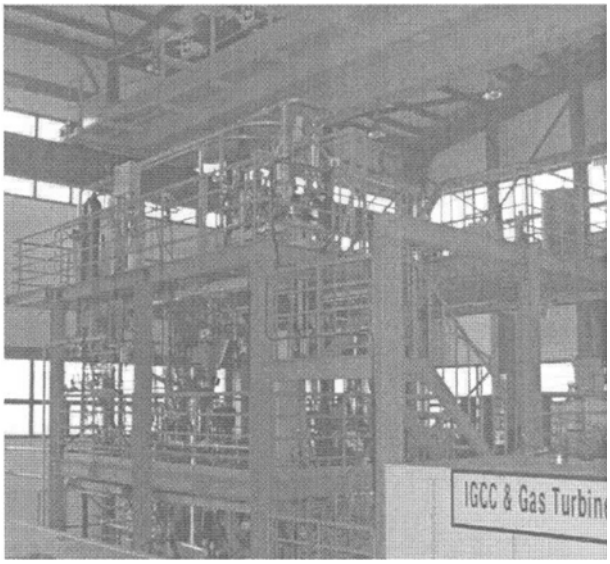

Fig. 3. One ton per day gasification system.

Table 2. The O_2 supply angle, linear velocity, and nozzle size of burners

Burner type	O_2 supply angle	Linear velocity	Nozzle size	Distance[a]
Type A	16°	100 m/s	φ1.6 mm×6	12 mm
Type B	7°	100 m/s	φ1.2 mm×10	25 mm

[a]Distance between the nozzle and the coal feeding hole

perature of 1,000 °C in atmospheric pressure. The gasifier is operated in these conditions for a sufficiently long time to ensure that a steady state is reached while the gas samples are collected for analysis.

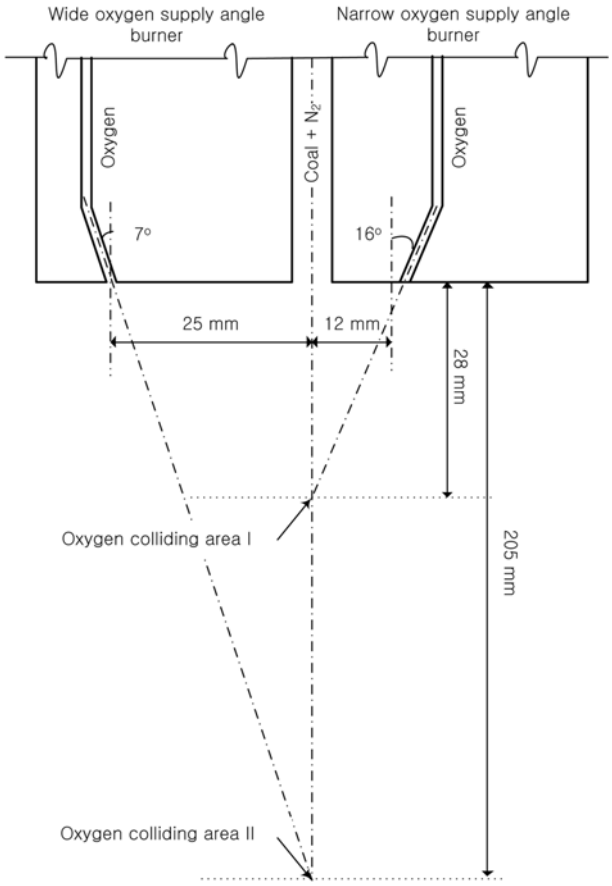

Fig. 4. Design drawing of each burner.

Table 3. Main elemental chemical composition (in wt%), high heating value (in kcal/kg), and elemental molar ratio of H/C and O/C for Adaro coal

Proximate analysis	% mass	Ultimate analysis	% mass
Fixed carbon	48.21	C	72.93
Volatile matter	43.33	H	5.21
Water	2.89	O	19.9
Ash	5.57	N	1.57
HHV (kcal/kg)	6578.8	S	0.28

Two burner types, A and B, were designed for the coal gasification tests. The main differences between the burners were the hole radius, nozzle angle, and oxygen supply distance from the coal feeding hole. The hole transferred the pulverized coal into the gasifier using high pressure nitrogen. The coal burner oxygen supply angles were 16° and 7° for type A and type B burners, respectively. The distances between the nozzle and the coal feeding hole were 12 mm and 25 mm, respectively. This difference can affect the location in which the coal meets the oxygen. The design specifications of these burners are described in Table 2 and illustrated in Fig. 4.

2. Experimental Results

The tests to discern the effect of the burner type were undertaken using Adaro coal; its proximate analysis and ultimate analysis are described in Table 3. The concentrations of CO, CO_2, H_2, carbon conversion, and gasifier temperature are plotted against the

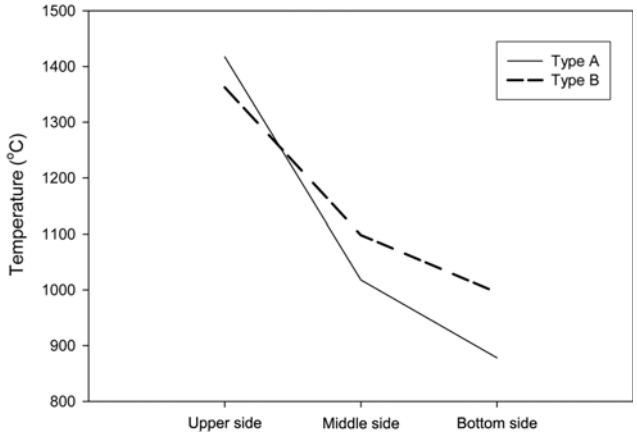

Fig. 5. Temperature profile depending on burner type.

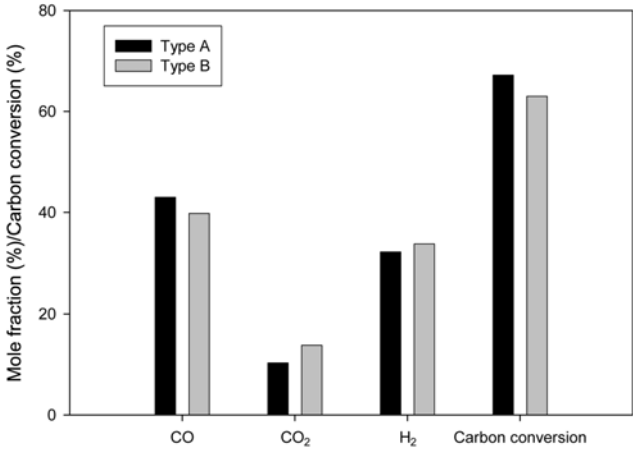

Fig. 6. Syngas composition depending on burner type.

two burner types in Fig. 5 and Fig. 6, and summarized in Table 4. These figures show that the burner types affect the syngas composition, carbon conversion, and gasifier temperature profile. The type A burner produced a higher temperature in the upper side than the type B burner and vice versa in the middle and the bottom sides. The concentration of CO was higher in the Type A burner, and the concentrations of CO_2 and H_2 were higher in the type B burner in the syngas stream.

Table 4. Experiment results

Condition	Type A	Type B
Pressure	3 bar	
Temp. of upper side	1417.4 °C	1362.6 °C
Temp. of middle side	1018.1 °C	1098.5 °C
Temp. of bottom side	878.2 °C	995.3 °C
Coal feed rate	40-45 kg/hr	
O_2/coal ratio	0.70-0.78	
N_2/coal ratio	0.40-0.45	
Syngas compositions & carbon conversion		
Component	Type A	Type B
CO* (mole fraction)	43.0%	39.8%
CO_2* (mole fraction)	10.3%	13.8%
H_2* (mole fraction)	32.3%	33.9%
Carbon conversion*	67.2%	63.0%

*Mean value of 512 data points for 27 minutes in a steady state

When the burner nozzle had a lower angle and was a long distance from the coal feeding hole, the possibility of reacting with the oxygen was lower in the upper side of the gasifier. As a result, the gasification zone was determined according to the burner type. This is evidenced by the higher temperatures and mole fraction of CO_2 at the middle and bottom sides of the gasifier, and the lower CO gas concentration in the syngas composition in the type B burner, as shown in Fig. 6 and Table 4, even though the inlet conditions were similar. Generally, gasification is composed of combustion and gasification reactions. The combustion reaction primarily generates CO_2, and the gasification reaction primary generates CO. Even though the combustion region and the gasification region are not clearly divided in entrained coal gasifiers, the combustion reaction is preferred over the gasification reaction in oxygen-rich regions. Furthermore, the combustion reaction is more exothermic than the gasification reaction. As shown in Fig. 4, the oxygen-rich oxygen collision areas of the narrow and wide oxygen supply angle burners were 28 mm and 205 mm apart from the burners respectively.

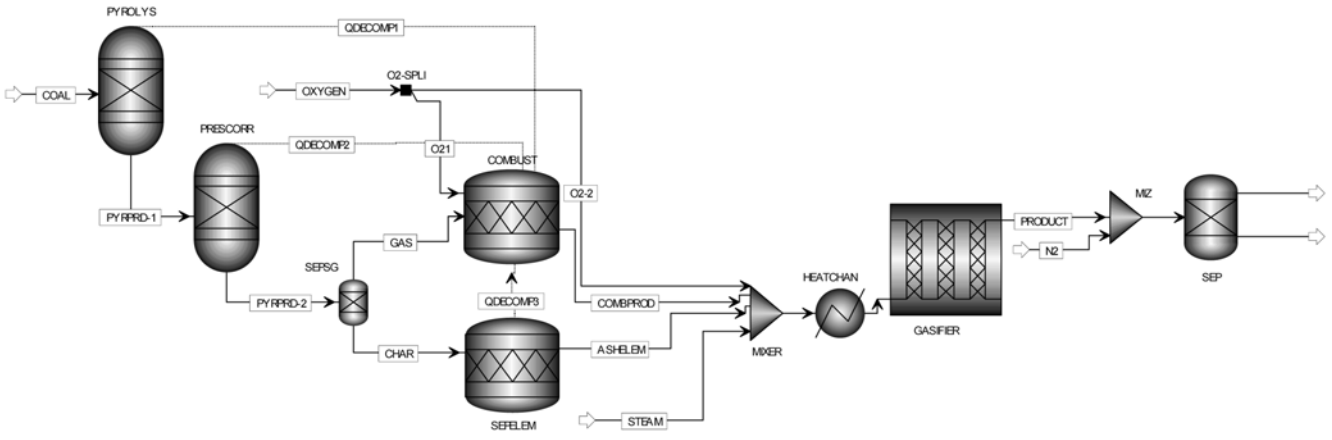

Fig. 7. Flow sheet for the coal gasification process.

The burner type determined the oxygen distribution pattern. In the type A burner, the gasification area was formed at a lower region than that in the type B burner because the oxygen collision area was formed at a lower region. Therefore, there were differences in the temperature profiles and syngas compositions.

3. Gasifier Model

Many mathematical models [2-4,6,8-11] have been developed to describe the different chemical reactions that occur in the gasifier. In this study, the gasifier model was developed in Aspen Plus and the subroutines were written in Fortran. Fig. 7 shows the flowsheet for the coal gasification process; it is divided into the main mechanisms in the gasifier. The model was modified with the considerations of heat loss to match the pilot plant system.

3-1. Coal Pyrolysis

In the gasifier, the temperature is typically higher than 1,000 °C. When coal is fed into the gasifier, it first undergoes a pyrolysis process to decompose to volatile matter, char, etc., as shown in Eq. (1) [2,18].

$$\text{Coal} \rightarrow \text{Char}+CO+H_2+H_2O+CO_2+CH_4+H_2S+N_2+\text{Tar} \quad (1)$$

This step is assumed to be instantaneous; thus, the interactions between the solid and gas are not considered.

3-2. Volatile Combustion

After the coal pyrolysis, the volatile material is composed of CO, H_2, CO_2, H_2O, H_2S, N_2, CH_4, and tar (assumed to be C_6H_6). Among these gases, CO, H_2, CH_4, and tar are combustible gases. Thus, after the coal pyrolysis, these combustible gases will react with the oxygen fed into the gasifier. Because the gases will be consumed quickly, the reaction kinetics of the volatile combustion process are neglected. The conversions of CO, H_2, and CO are assumed to be 100% [18].

$$\text{Tar}(C_6H_6)+7.5O_2 \rightarrow 6CO_2+3H_2O \quad (2)$$

$$H_2+0.5O_2 \rightarrow H_2O \quad (3)$$

$$CO+0.5O_2 \rightarrow H_2O \quad (4)$$

$$CH_4+2O_2 \rightarrow CO_2+2H_2O \quad (5)$$

3-3. Char Gasification

Wen and Chang [2] suggested the reaction as below Eq. (6).

$$C+\left(\frac{1}{\phi}\right)O_2 \rightarrow 2\left(1-\frac{1}{\phi}\right)CO+\left(\frac{2}{\phi}-1\right)CO_2 \quad (6)$$

In this reaction, ϕ is a coefficient that depends on the diameter of the coal particle (d_p) and can be calculated using the relations in Table 5.

For a given temperature, ϕ is constant at d_p<0.005 cm and d_p> 0.1 cm. At 0.005≤0.01 cm, ϕ decreases with the increase in d_p. For a given d_p, ϕ shows a slight change with the temperature at d_p≤0.1 cm. At d_p>0.1 cm, ϕ is independent of the temperature and has a value of 1.0. These reaction characteristics can be understood because the frequency of the reaction of the coal particles with oxygen depends on the particle size.

Table 5. Expression of for different coal particle size [2,18]

d_p	ϕ	Comment
<0.005	$\frac{2Z+2}{Z+2}$	
0.005-0.1	$\frac{(2Z+2)-\frac{Z(d_p-0.005)}{0.095}}{Z+2}$	$Z=\frac{[CO]}{[CO_2]}=2500e^{-\frac{6249}{T}}$
>0.1	1	

After the volatile combustion process, the char from the coal pyrolysis is further gasified using the gases in the gas phase. This process may include the reactions presented in Eq. (7) to Eq. (12) below, as well as reactions presented in Eq. (2) to Eq. (6) above.

$$C+H_2O \rightarrow CO+H_2 \quad (7)$$

$$C+CO_2 \rightarrow 2CO \quad (8)$$

$$C+2H_2 \rightarrow CH_4 \quad (9)$$

$$S+H_2 \rightarrow H_2S \quad (10)$$

$$CH_4+H_2O \leftrightarrow CO+3H_2 \quad (11)$$

$$CO+H_2O \leftrightarrow CO_2+H_2 \quad (12)$$

The unreacted-core shrinking model is used to describe the kinetics. In this model, the effects of the ash layer diffusion, gas film diffusion and chemical reaction are considered. The overall rate is expressed as in Eq. (13). All reactions are modeled with parameters from the literature [2,18].

$$R_{c-i}=\frac{1}{\frac{1}{k_{diff}}+\frac{1}{k_s Y^2}+\frac{1}{k_{dash}\left(\frac{1}{Y}-1\right)}}(P_i-P_i^*) \quad (13)$$

where

k_{diff} : gas film diffusion constant, g/cm^2·atm·s;

k_s : surface reaction constant, g/cm^2·atm·s; and

k_{dash} : gas film diffusion constant, g/cm^2·atm·s, $k_{dash}=k_{diff}\cdot e^n$ where ε is a voidage in the gas layer; and n is a constant ranging from 2 to 3.

$Y=(r_c/r_p)=((1-x)/(1-f))^{1/3}$, where r_c is the radius of the unreacted core, r_p is the radius of the whole particle including the ash layer, x is the coal conversion at any time after the pyrolysis is complete, and f is the coal conversion when the pyrolysis is complete.

$P_i-P_i^*$ is the effective particle pressure of *i*-component considering the reverse reaction

The kinetics of the reactions (Eqs. (6) to (10)) are shown in Table 6 [18]. The kinetics of the reactions presented in Eqs. (3) to (5), (11), and (12) are shown in Table 7 [18].

3-4. Developed Gasification Reactor Model

The developed model was modified with the considerations of heat loss to match the pilot plant system. To consider the heat loss in the simulation model, a heat-exchanger based on the experimental results was used. To comprise burner types, the temperature was changed by changing the residence time. The changes in the temperature profile according to the burner type can be explained by the change in the gasification area size.

RESULT COMPARISON AND DISCUSSION

1. Result Comparison

In the general simulation model, the gasification temperature is considered to be independent of other conditions. In this case, the

Table 6. Parameters for kinetic reactions [18]

Reaction	k_{diff}	k_s	$P_i - P_i^*$	k_{eq}
(6)	$\frac{0.292\phi\left(\frac{4.26}{T}\right)\left(\frac{T}{1800}\right)^{1.75}}{P_t d_p}$	$8710e^{-\frac{17967}{T}}$	P_{O_2}	
(7)	$\frac{10\times10^{-4}\left(\frac{T}{2000}\right)^{0.75}}{P_t d_p}$	$247e^{-\frac{21060}{T}}$	$P_{H_2O}-\frac{P_{H_2}P_{CO}}{K_{eq}}$	$e^{17.644-\frac{30260}{1.8T}}$
(8)	$\frac{7.45\times10^{-4}\left(\frac{T}{2000}\right)^{0.75}}{P_t d_p}$	$247e^{-\frac{21060}{T}}$	P_{CO_2}	
(9)	$\frac{1.33\times10^{-3}\left(\frac{T}{2000}\right)^{0.75}}{P_t d_p}$	$0.12e^{-\frac{1792.1}{T}}$	$P_{H_2}-\sqrt{\frac{P_{CH_4}}{K_{eq}}}$	$\frac{0.175}{34173}e^{\frac{18400}{1.8T}}$
(10)	$\frac{1.33\times10^{-3}\left(\frac{T}{2000}\right)^{0.75}}{P_t d_p}$	$0.12e^{-\frac{1792.1}{T}}$	$P_{H_2}-\frac{P_{H_2S}}{K_{eq}}$	$e^{-5.0657+\frac{18557.7}{T}}$

Table 7. Kinetics of reactions [18]

Reaction	Reaction rate	Comment	Unit
(3)	$8.83\times10^5 e^{-\frac{9.976\times10^4}{8.315T}} C_{H_2}C_{O_2}$		$mol/m^3\cdot s$
(4)	$30.9e^{-\frac{9.976\times10^4}{8.315T}} C_{CO}C_{O_2}$		$mol/m^3\cdot s$
(5)	$3.552\times10^{11} e^{-\frac{9.304\times10^4}{8.315T}} C_{CH_4}C_{O_2}$		$mol/m^3\cdot s$
(11)	$312e^{-\frac{30000}{1.987T}}\left(C_{CH_4}-\frac{C_{CO}C_{H_2}^3}{K_{eq}\cdot C_{H_2O}}\right)$	$K_{eq}=e^{33.1-\frac{250.14}{T}}$	$mol/m^3\cdot s$
(12)	$F_w\cdot2.77\cdot10^5(x_{CO}-x_{CO}^*)e^{-\frac{27760}{1987T}}\cdot P_t^{0.5-\frac{P_t}{250}}\cdot e^{-8.91+\frac{5553}{T}}$	$x_{CO}=\frac{P_{CO}}{P_t}$ $x_{CO}^*=\frac{1}{P_t}\cdot\frac{P_{CO_2}P_{H_2}}{K_{eq}P_{H_2O}}$ $K_{eq}=e^{-3.7+\frac{7234}{1.8T}}$	$mol/[s\cdot ash(g)]$

syngas compositions as functions of the oxygen-to-coal ratio can be found at fixed temperatures. Using Gibbs reactor in the model is a useful exercise for equilibrium evaluations but is not suitable for practical applications. In real reactors, changes in the oxygen in the feed and other input changes create higher or lower temperatures in the gasifier. Thus, these are not independent of each other. To simulate real gasifier behavior, the reactor was not adopted at fixed temperature in this simulation. The global heat balance included the reaction heat at each step: pyrolysis, combustion, and gasification reaction. This may affect the efficiency and syngas compositions.

First, a type A burner model was fabricated. After the comparison between the experimental and simulation results from the type A burner, the model was modified to meet the experimental data from the type B burner.

The comparisons of the syngas composition and temperature from the experimental results and simulation results using the type A burner shown in Figs. 8, 9 and Table 8. The simulation results agreed

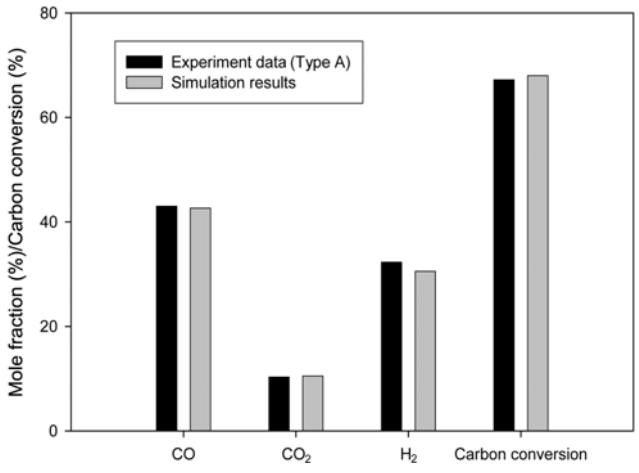

Fig. 8. Comparison between the experimental data (Type A) and simulation results.

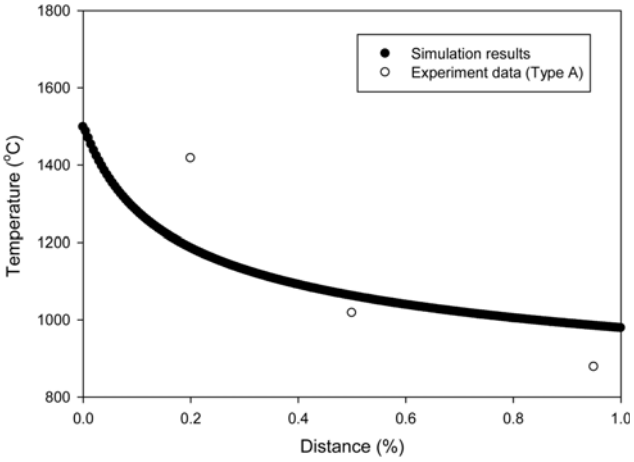

Fig. 9. Temperature profile of the gasifier (Type A) and simulation results.

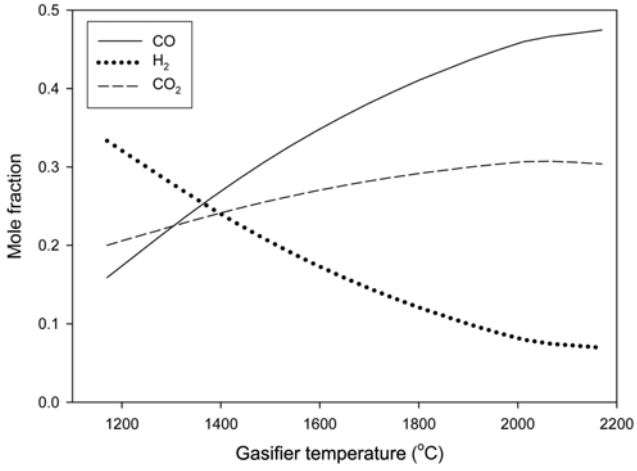

Fig. 10. Component composition with gasifier temperature.

Table 8. Comparison between the experimental data and simulation results

Condition	Experimental data (Type A)	Simulation results
Pressure	3 bar	
Maximum temperature	1417.4 °C	1498.1 °C
Coal feed rate	40-45 kg/hr	45 kg/hr
O_2/coal ratio	0.70-0.78	0.78
N_2/coal ratio	0.40-0.45	0.45
Syngas compositions & carbon conversion		
Component	Experimental data (Type A)	Simulation results
CO (mole fraction)	43.0%	42.6%
CO_2 (mole fraction)	10.3%	10.5%
H_2 (mole fraction)	32.3%	30.5%
Carbon conversion	67.2%	68%

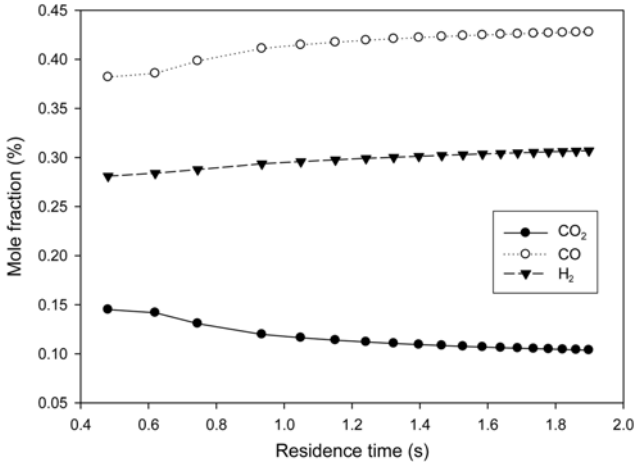

Fig. 11. Change of component composition with residence time.

well with the experimental results, excepting the temperature profile: the simulation generated higher temperatures than the experiment. There are two probable causes for this variation in the results. The first could be the combustion heat of the coal. In this model, the combustion heat was calculated using Boie correlation in Aspen Plus. The value had a significant effect on the enthalpy of the coal. An inaccurate value might cause an incorrect enthalpy of coal and consequently an incorrect gasifier temperature. If the combustion heat was obtained experimentally, the value in Aspen Plus could be modified. Another cause for variation could be that the model was simulated in an adiabatic mode. To consider the heat loss in the simulation model and to adjust the simulation model to the experimental results, a heat-exchanger based on the experimental results was used. Furthermore, the kinetics data were not well matched with those of the bench gasifier, including the effects of the coal properties. Even though the kinetic data could be modified to fit the experimental results, it is not a meaningful process or reasonable estimate, but rather it is only a tuning process without scientific basis. For these reasons, there was a gap in the maximum temperature between the experimental data and simulation results.

In the next step, the simulation was modified to accommodate the type B burner results. The difference between the burner types in the experimental results was the temperature profile and syngas composition. To confirm the relationship between the temperature and syngas composition, a sensitivity analysis was performed. The dependency of the compositions on the gasifier temperature in this simulation is shown in Fig. 10. The hydrogen and carbon monoxide concentrations increased and the carbon dioxide concentration decreased when the temperature increased in the simulation. This agreed well with the experimental data.

Based on these results, the temperature was changed by changing the residence time. The changes in the temperature profile according to the burner type can be explained by the change in the gasification area size. The temperature in the gasification zone under a relatively higher oxygen concentration is much higher. As a result, the gasification zone and residence time change depending on the burner type. To simulate the difference in the burner type, the reactor size was changed in the simulation, which resulted in a change in the residence time in the simulation. The syngas composition change according to the residence time change in the simulation is shown

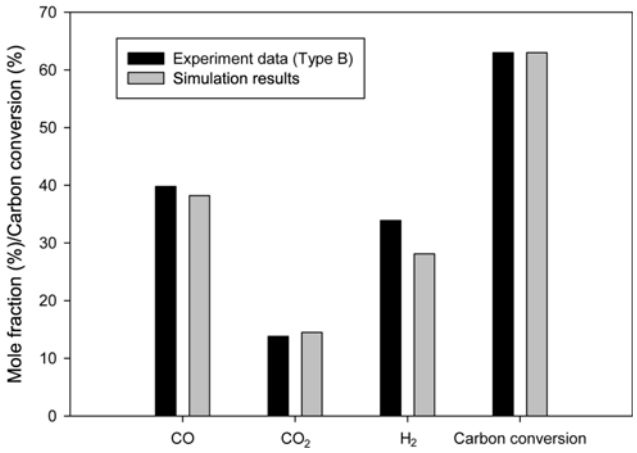

Fig. 12. Comparison between experimental data (Type B) and simulation results.

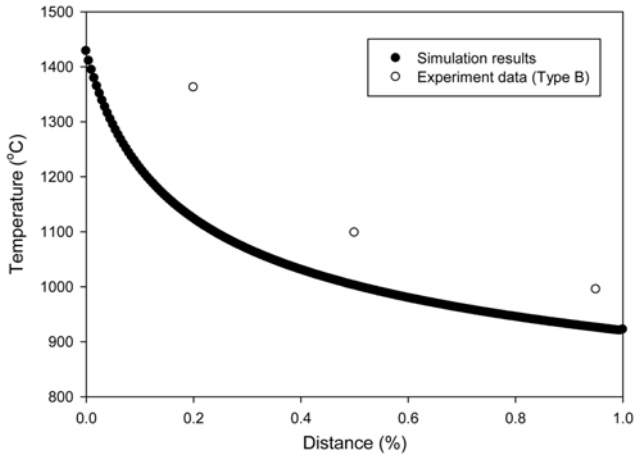

Fig. 13. Temperature profile of gasifier (Type B) and simulation results.

in Fig. 11. The gasifier with a shorter residence time had higher CO_2 and lower CO concentrations. The trends in the simulation agreed well with the experimental results.

Comparisons of the syngas composition and temperature in the experimental results using the type B burner with the simulation results are shown in Fig. 12, Fig. 13 and Table 9. The results agreed with experimental results as with those of the type A burner. Table 10 shows the differences between the simulation models.

2. Optimal Operating Conditions

Based on these results, the more appropriate burner type for the proposed system could be determined. The type A burner showed better results: the effects of the operating conditions on the syngas composition were evaluated to optimize the gasifier performance in the bench gasifier facility. The coal feed rate and coal properties were maintained constant in all simulations, while the oxygen to coal ratio could be varied in wide range (0.7-1.1).

For this simulation, an optimal region was observed near an oxygen feed rate of 39-45 kg/hr, where the concentrations of CO and H_2 were highest as shown in Fig. 14. To obtain better results in the bench gasifier, the oxygen flow rate needed to be increased within the oxygen to coal ratio (around 0.87). The result is shown in Fig. 14.

Table 9. Comparison between experimental data and simulation results

Condition	Experimental data (Type B)	Simulation results
Pressure	3 bar	
Maximum temperature	1362.6 °C	1428.6 °C
Coal feed rate	40-45 kg/hr	45 kg/hr
O_2/coal ratio	0.70-0.78	0.78
N_2/coal ratio	0.40-0.45	0.45
Syngas compositions & carbon conversion		
Component	Experimental data (Type B)	Simulation results
CO (mole fraction)	39.8%	38.2%
CO_2 (mole fraction)	13.8%	14.5%
H_2 (mole fraction)	33.9%	28.1%
Carbon conversion	63.0%	63.0%

Table 10. Comparison between simulation results

Condition	Simulation results (Type A)	Simulation results (Type B)
Pressure	3 bar	
Maximum temperature	1417.4 °C	1428.6 °C
Residence time	1.68 Seconds	0.48 Seconds
Coal feed rate	40-45 kg/hr	45 kg/hr
O_2/coal ratio	0.70-0.78	0.78
N_2/coal ratio	0.40-0.45	0.45
Syngas compositions & carbon conversion		
Component	Simulation results (Type A)	Simulation results (Type B)
CO (mole fraction)	43.0%	38.2%
CO_2 (mole fraction)	10.3%	14.5%
H_2 (mole fraction)	32.3%	28.1%
Carbon conversion	67.2%	63.0%

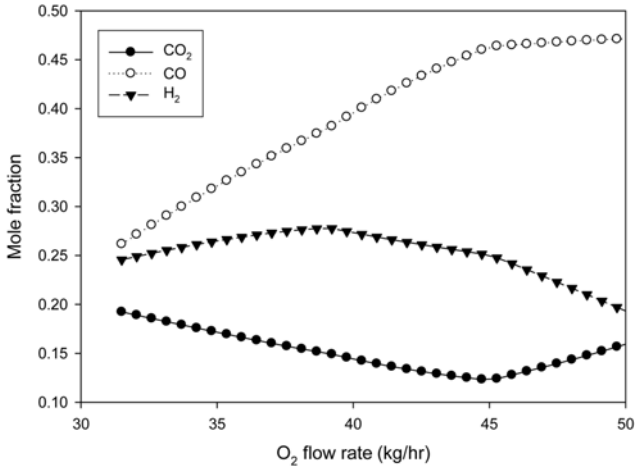

Fig. 14. Component composition and temperature with oxygen flow rate.

CONCLUSIONS

This study presents the experimental and simulation results of an IGCC bench-scale process, focusing on entrained bed gasification for syngas production. The effect of two different burner types for the gasifier on the gas composition, carbon conversion, and gasifier temperature were investigated through experiments and simulations using the Aspen Plus process simulator.

Gasifier characteristics that are difficult to measure in the actual gasifier were predicted well using the developed model. The trends of the basic gasification parameters, such as the component concentration, cold gas efficiency, and thermal behavior of gasifier, were predicted. It was confirmed that most features of the gasification performance that change under different operating conditions were tested by the developed model. The present model can be effectively used as a tool to obtain the optimal operating conditions in bench-scale gasifier and supporting general entrained coal gasifier operation by incorporating the predicted data. For future work, developing gasifier models using the procedure described in this study will allow different reactor configurations to be compared.

ACKNOWLEDGEMENTS

This work was supported by Development of Operation Technologies for Korea 300 MW IGCC plant of the Korea Institute of Energy Technology Evaluation and Planning (KETEP) grant funded by the Korea government Ministry of Knowledge Economy (No. 2011951010001C).

REFERENCES

1. Future Development of IGCC, IEA Clean Coal Center (2008).
2. C. Y. Wen and T. Z. Chaung, *Ind. Eng. Chem. Process Des. Dev.*, **18**, 684 (1979).
3. R. Govind and J. Shah, *AIChE J.*, **30**(1), 79 (1984).
4. C. Higman and M. Van der Burgt, 2nd Ed., Elsevier (2003).
5. C. H. Frey and N. Akunuri, http://www4.ncsu.edu/~frey/reports/Frey_akunuri_2001.pdf (2001).
6. E. Martinez, W. Vicente and M. Salinas Vazquez, *Information Technology*, **6**, 141 (2006).
7. S. V. Nathe, R. D. Kirkpatrick and B. R. Young, *Energy Fuels*, **22**, 2687 (2008).
8. C. Chen, M. Horio and T. Kojima, *Chem. Eng. Sci.*, **55**, 3861 (2000).
9. D. Brown, T. Fuchino and F. Marechal, Elsevier, 1661 (2005).
10. A. Valero and S. Uson, *Energy*, **28**, 7433 (2003).
11. I. Petersen and J. Werther, *Chem. Eng. Sci.*, **44**, 717 (2005).
12. P. J. Robinson and W. L. Luyben, *Ind. Eng. Chem. Res.*, **47**, 7784 (2008).
13. E. Biagini, A. Bardi, G Pannocchia and L. Tognotti, *Ind. Eng. Chem. Res.*, **48**, 9028 (2009).
14. M Perez-Fortes, A. D. Bojarski, E. Velo, J. M. Nougues and L. Puigjaner, *Energy*, **34**, 1721 (2009).
15. J. W. Lee, M. Y. Kim, J. H. Chi, S. M. Kim and S. I. Park, *Trans. of the Korean Hydrogen and New Energy Society*, **21**, 425 (2010).
16. S. I. Park, J. W. Lee, and H. K. Seo, *Transactions of the Korean Hydrogen and New Energy Society*, **21**, 470 (2010).
17. S. I. Park, J. W. Lee, H. K. Seo, G. S. Kim and K. T. Kim, *Fuel Processing Technology*, 7, 1374 (2011).
18. Aspen Technology, Inc. Aspen Plus Model for Entrained Flow Coal Gasifier, V7.2, http://support.aspentech.com.